SCIENCE CHINA
Physics, Mechanics & Astronomy

• Research Paper •
Special Issue: Forward for the Department of Engineering Mechanics, Tsinghua University

April 2011 Vol.54 No.4: 653–665
doi: 10.1007/s11433-011-4272-6

Shape-free finite element method: The plane hybrid stress-function (HS-F) element method for anisotropic materials

CEN Song[1,4*], FU XiangRong[2], ZHOU GuoHua[1], ZHOU MingJue[1] & LI ChenFeng[3]

[1]*Department of Engineering Mechanics, School of Aerospace, Tsinghua University, Beijing 100084, China;*
[2]*College of Water Conservancy & Civil Engineering, China Agricultural University, Beijing 100083, China;*
[3]*Civil & Computational Engineering Centre, School of Engineering, Swansea University, Swansea, SA2 8PP, UK;*
[4]*Key laboratory of Applied Mechanics, School of Aerospace, Tsinghua University, Beijing 100084, China*

Received November 30, 2010; accepted January 19, 2011; published online February 15, 2011

The sensitivity problem to mesh distortion and the low accuracy problem of the stress solutions are two inherent difficulties in the finite element method. By applying the fundamental analytical solutions (in global Cartesian coordinates) to the Airy stress function ϕ of the anisotropic materials, 8- and 12-node plane quadrilateral hybrid stress-function (HS-F) elements are successfully developed based on the principle of the minimum complementary energy. Numerical results show that the present new elements exhibit much better and more robust performance in both displacement and stress solutions than those obtained from other models. They can still perform very well even when the element shapes degenerate into a triangle and a concave quadrangle. It is also demonstrated that the proposed construction procedure is an effective way for developing shape-free finite element models which can completely overcome the sensitivity problem to mesh distortion and can produce highly accurate stress solutions.

finite element, hybrid stress-function (HS-F) element, shape-free, stress function, the principle of minimum complementary energy, fundamental analytical solutions, anisotropic materials

PACS: 02.70.-c, 02.70.Dc, 46.15.-x, 46.25.-y

1 Introduction

The finite element method is a widely-used numerical tool in modern computations and simulations for engineering and science [1,2]. However, such a powerful method still suffers from some numerical problems that have not been well solved. For example, once the element mesh is distorted, the accuracy of the numerical results may descend dramatically. This is the sensitivity problem to mesh distortion [3]. For another example, because of the inherent theoretical defects of the displacement-based element models, the convergence for the stress solutions is usually not as good as that for displacement solutions. Over the past 50 years, numerous techniques have been proposed for developing robust finite element models which are insensitive to mesh distortion, such as the incompatible displacement modes [4–6], the enhanced strain method [7], the stabilization method [8], the selectively reduced integration scheme [9], the assumed strain formulations [10,11], the quasi-conforming element method [12], the generalized conforming method [13], the Alpha finite element method [14], the new spline finite element method [15], the unsymmetric interpolation method [16–18], the new natural coordinate methods [19–24], and so on. Although the above schemes can improve the robustness of the finite elements more or less, it should be noted that most models will fail once the element shape is severely distorted, such as the situation that a convex quadrangle degenerates into a triangle or a concave quadrangle. Hence, many researchers have to look

*Corresponding author (email: censong@tsinghua.edu.cn)

for various meshfree or meshless methods [25–29] which require much higher computational costs.

Recently, by simply improving the first version of the hybrid stress element method proposed by Pian [30], Fu and Cen [31,32] proposed a hybrid stress-function (HS-F) element method which is immune to severely distorted mesh containing elements with concave shapes. Firstly, the stress function ϕ is regarded as the functional variable and introduced into the complementary energy functional. Secondly, the fundamental analytical solutions (in global Cartesian coordinates) of ϕ to the isotropic plane problem are taken as the trial functions. Thus, the resulting stress fields must be reasonable because all system governing equations, including the equilibrium and the compatibility relations, can be satisfied. Thirdly, by applying the principle of minimum complementary energy, the unknown stress-function parameters can be expressed in terms of the displacements along element boundaries, which can be interpolated directly by the element nodal displacements. Finally, the complementary energy functional can be rewritten in terms of element nodal displacement vector, and thus, the element stiffness matrix of such a HS-F element is obtained. The plane quadrilateral finite element models developed by following the above procedure exhibit excellent performance in both regular and distorted meshes, even when the element shape degenerates into a triangle or a concave quadrangle. Since all field equations for the elastic problem can be satisfied within one element, the HS-F element method is somewhat similar to the hybrid-Trefftz stress element method [33–35]. But, they are quite different in the theoretical basis, the element technique, and the fundamental solutions used as the trial functions. Actually, the HS-F element method is simpler and more straightforward.

The fundamental solutions used in the HS-F elements and the hybrid-Trefftz stress elements are all only for isotropic materials, which limits the applications of these high performance element methods. The main purpose of this paper is to break through such a limitation and establish a frame of the plane HS-F element method for anisotropic materials. This paper is outlined as follows. Firstly, the constitutive relations for the anisotropic materials of the plane linearly elastic problems are given in sect. 2. Then, twenty-three fundamental analytical solutions (in global Cartesian coordinates) to the Airy stress function ϕ of the anisotropic materials, which are not found in the literature, are presented in sect. 3. And the formulations of 8- and 12-node plane quadrilateral HS-F elements for anisotropic materials are developed in sect. 4. The results of some meaningful benchmark problems are reported in sect. 5. The proposed elements exhibit excellent performance for both stress and displacement solutions in various numerical examples, even when the element shape degenerates into a triangle and a concave quadrangle. Hence, they are a kind of shape-free finite element models which can completely overcome the sensitivity problem to mesh distortion and can produce highly accurate stress solutions.

2 Constitutive relations for plane linearly elastic problems

For a plane linearly elastic problem of anisotropic materials, the direction normal to the plane of deformation (i.e., the z direction) must be a direction of material symmetry. The constitutive relations, also known as strain-stress or stress-strain equations, can be expressed by (ignoring the initial stresses and strains)

$$\begin{Bmatrix}\sigma_x\\ \sigma_x\\ \sigma_z\\ \tau_{xy}\end{Bmatrix}=\begin{bmatrix}D_{11} & D_{12} & D_{13} & D_{16}\\ D_{21} & D_{22} & D_{23} & D_{26}\\ D_{31} & D_{32} & D_{33} & D_{36}\\ D_{61} & D_{62} & D_{63} & D_{66}\end{bmatrix}\begin{Bmatrix}\varepsilon_x\\ \varepsilon_y\\ \varepsilon_z\\ \gamma_{xy}\end{Bmatrix}, \tag{1a}$$

$$\begin{Bmatrix}\varepsilon_x\\ \varepsilon_y\\ \varepsilon_z\\ \gamma_{xy}\end{Bmatrix}=\begin{bmatrix}C_{11} & C_{12} & C_{13} & C_{16}\\ C_{21} & C_{22} & C_{23} & C_{26}\\ C_{31} & C_{32} & C_{33} & C_{36}\\ C_{61} & C_{62} & C_{63} & C_{66}\end{bmatrix}\begin{Bmatrix}\sigma_x\\ \sigma_x\\ \sigma_z\\ \tau_{xy}\end{Bmatrix}, \tag{1b}$$

where $D_{ij}=D_{ji}$, $C_{ij}=C_{ji}$ (i,j=1,2,3,6) are elastic moduli and compliances, respectively, and

$$\begin{bmatrix}C_{11} & C_{12} & C_{13} & C_{16}\\ C_{21} & C_{22} & C_{23} & C_{26}\\ C_{31} & C_{32} & C_{33} & C_{36}\\ C_{61} & C_{62} & C_{63} & C_{66}\end{bmatrix}=\begin{bmatrix}D_{11} & D_{12} & D_{13} & D_{16}\\ D_{21} & D_{22} & D_{23} & D_{26}\\ D_{31} & D_{32} & D_{33} & D_{36}\\ D_{61} & D_{62} & D_{63} & D_{66}\end{bmatrix}^{-1}. \tag{2}$$

For the plane stress case we must set $\sigma_z=0$. Then, from eq. (1a), ε_z can be solved as:

$$\varepsilon_z=-\left(D_{31}\varepsilon_x+D_{32}\varepsilon_y+D_{36}\gamma_{xy}\right)\Big/D_{33}, \tag{3}$$

which may be substituted into eq. (1a) to give

$$\begin{Bmatrix}\sigma_x\\ \sigma_x\\ \sigma_z\\ \tau_{xy}\end{Bmatrix}=\begin{bmatrix}\hat{D}_{11} & \hat{D}_{12} & 0 & \hat{D}_{16}\\ \hat{D}_{21} & \hat{D}_{22} & 0 & \hat{D}_{26}\\ 0 & 0 & 0 & 0\\ \hat{D}_{61} & \hat{D}_{62} & 0 & \hat{D}_{66}\end{bmatrix}\begin{Bmatrix}\varepsilon_x\\ \varepsilon_y\\ \varepsilon_z\\ \gamma_{xy}\end{Bmatrix}, \tag{4}$$

in which

$$\hat{D}_{ij}=D_{ij}-D_{i3}D_{33}^{-1}D_{3j},\quad (i,j=1,2,6) \tag{5}$$

are reduced elastic moduli. Thus, we have

$$\boldsymbol{\varepsilon}=\begin{Bmatrix}\varepsilon_x\\ \varepsilon_y\\ \gamma_{xy}\end{Bmatrix}=\begin{bmatrix}\hat{D}_{11} & \hat{D}_{12} & \hat{D}_{16}\\ \hat{D}_{21} & \hat{D}_{22} & \hat{D}_{26}\\ \hat{D}_{61} & \hat{D}_{62} & \hat{D}_{66}\end{bmatrix}^{-1}\begin{Bmatrix}\sigma_x\\ \sigma_y\\ \tau_{xy}\end{Bmatrix}$$

$$= \begin{bmatrix} \hat{C}_{11} & \hat{C}_{12} & \hat{C}_{16} \\ \hat{C}_{21} & \hat{C}_{22} & \hat{C}_{26} \\ \hat{C}_{61} & \hat{C}_{62} & \hat{C}_{66} \end{bmatrix} \begin{Bmatrix} \sigma_x \\ \sigma_y \\ \tau_{xy} \end{Bmatrix} = \boldsymbol{C}\boldsymbol{\sigma}, \tag{6}$$

where $\boldsymbol{C}$ is the elasticity matrix of compliances.

For the plane strain case we must set $\varepsilon_z = 0$. Then, from eq. (1b), σ_z can be solved as:

$$\sigma_z = -\left(C_{31}\sigma_x + C_{32}\sigma_y + C_{36}\tau_{xy}\right)\Big/C_{33}, \tag{7}$$

which may be substituted into eq. (1b) to give

$$\begin{Bmatrix} \varepsilon_x \\ \varepsilon_y \\ \varepsilon_z \\ \gamma_{xy} \end{Bmatrix} = \begin{bmatrix} \hat{C}_{11} & \hat{C}_{12} & 0 & \hat{C}_{16} \\ \hat{C}_{21} & \hat{C}_{22} & 0 & \hat{C}_{26} \\ 0 & 0 & 0 & 0 \\ \hat{C}_{61} & \hat{C}_{62} & 0 & \hat{C}_{66} \end{bmatrix} \begin{Bmatrix} \sigma_x \\ \sigma_x \\ \sigma_z \\ \tau_{xy} \end{Bmatrix}, \tag{8}$$

in which $\hat{C}_{ij} = C_{ij} - C_{i3}C_{33}^{-1}C_{3j}, \quad (i, j = 1, 2, 6)$ (9)

are reduced elastic compliances. Thus, we have

$$\boldsymbol{\varepsilon} = \begin{Bmatrix} \varepsilon_x \\ \varepsilon_y \\ \gamma_{xy} \end{Bmatrix} = \begin{bmatrix} \hat{C}_{11} & \hat{C}_{12} & \hat{C}_{16} \\ \hat{C}_{21} & \hat{C}_{22} & \hat{C}_{26} \\ \hat{C}_{61} & \hat{C}_{62} & \hat{C}_{66} \end{bmatrix} \begin{Bmatrix} \sigma_x \\ \sigma_y \\ \tau_{xy} \end{Bmatrix} = \boldsymbol{C}\boldsymbol{\sigma}, \tag{10}$$

For orthotropic materials, it is common to define their properties in terms of their Young's moduli, Poisson ratios and shear moduli. Let x' and y' be the two axes of material symmetry in the plane of deformation, and the elastic strain-stress relations may be expressed by

$$\begin{Bmatrix} \varepsilon_{x'} \\ \varepsilon_{y'} \\ \varepsilon_{z'} \\ \gamma_{x'y'} \end{Bmatrix} = \begin{bmatrix} \dfrac{1}{E_{x'}} & -\dfrac{\mu_{x'y'}}{E_{y'}} & -\dfrac{\mu_{x'z'}}{E_{z'}} & 0 \\ -\dfrac{\mu_{y'x'}}{E_{x'}} & \dfrac{1}{E_{y'}} & -\dfrac{\mu_{y'z'}}{E_{z'}} & 0 \\ -\dfrac{\mu_{z'x'}}{E_{x'}} & -\dfrac{\mu_{z'y'}}{E_{y'}} & \dfrac{1}{E_{z'}} & 0 \\ 0 & 0 & 0 & \dfrac{1}{G_{x'y'}} \end{bmatrix} \begin{Bmatrix} \sigma_{x'} \\ \sigma_{y'} \\ \sigma_{z'} \\ \tau_{x'y'} \end{Bmatrix}. \tag{11}$$

After the symmetry is considered, the number of independent components is reduced to seven parameters (three direct moduli, three Poisson ratios, and one shear modulus). Then, we have

$$\boldsymbol{\varepsilon}' = \begin{Bmatrix} \varepsilon_{x'} \\ \varepsilon_{y'} \\ \gamma_{x'y'} \end{Bmatrix} = \begin{bmatrix} \hat{C}'_{11} & \hat{C}'_{12} & \hat{C}'_{16} \\ \hat{C}'_{21} & \hat{C}'_{22} & \hat{C}'_{26} \\ \hat{C}'_{61} & \hat{C}'_{62} & \hat{C}'_{66} \end{bmatrix} \begin{Bmatrix} \sigma_{x'} \\ \sigma_{y'} \\ \tau_{x'y'} \end{Bmatrix} = \boldsymbol{C}'\boldsymbol{\sigma}', \tag{12}$$

in which $\boldsymbol{C}' = \begin{bmatrix} \dfrac{1}{E_{x'}} & -\dfrac{\mu_{x'y'}}{E_{y'}} & 0 \\ -\dfrac{\mu_{y'x'}}{E_{x'}} & \dfrac{1}{E_{y'}} & 0 \\ 0 & 0 & \dfrac{1}{G_{x'y'}} \end{bmatrix}$ (13)

for the plane stress case, and

$$\boldsymbol{C}' = \begin{bmatrix} \dfrac{1-\mu_{x'z'}\mu_{z'x'}}{E_{x'}} & -\dfrac{\mu_{x'y'}+\mu_{x'z'}\mu_{z'y'}}{E_{y'}} & 0 \\ -\dfrac{\mu_{y'x'}+\mu_{y'z'}\mu_{z'x'}}{E_{x'}} & \dfrac{1-\mu_{y'z'}\mu_{z'y'}}{E_{y'}} & 0 \\ 0 & 0 & \dfrac{1}{G_{x'y'}} \end{bmatrix} \tag{14}$$

for the plane strain case. Finally, the elasticity matrix of compliances in the global *xoy* coordinate system (see Figure 1), $\boldsymbol{C}$, can be expressed by

$$\boldsymbol{C} = \boldsymbol{T}^{\mathrm{T}}\boldsymbol{C}'\boldsymbol{T}, \tag{15}$$

$$\boldsymbol{T} = \begin{bmatrix} \cos^2\theta & \sin^2\theta & 2\sin\theta\cos\theta \\ \sin^2\theta & \cos^2\theta & -2\sin\theta\cos\theta \\ -\sin\theta\cos\theta & \sin\theta\cos\theta & \cos^2\theta - \sin^2\theta \end{bmatrix}. \tag{16}$$

And for isotropic materials, the elasticity matrix of compliances may be expressed by

$$\boldsymbol{C} = \frac{1}{E'}\begin{bmatrix} 1 & -\mu' & 0 \\ -\mu' & 1 & 0 \\ 0 & 0 & 2\left(1+\mu'\right) \end{bmatrix}, \tag{17}$$

in which $E'=E$ and $\mu'=\mu$ for the plane stress problem, and $E'=E/(1-\mu^2)$ and $\mu'=\mu/(1-\mu)$ for the plane strain problem. E and μ are Young's modulus and Poisson's ratio, respectively.

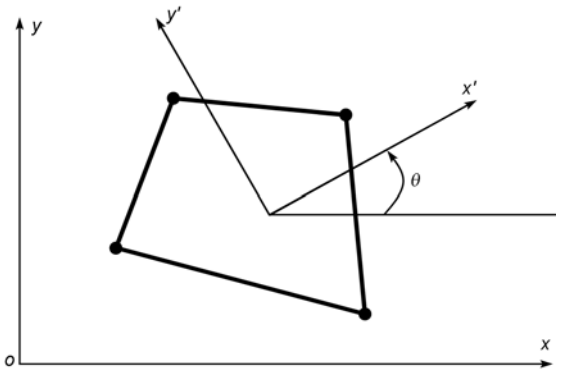

Figure 1 Coordinate definition for the transformation of material axes.

It should be noted that the elasticity matrix of compliances $\boldsymbol{C}$ is always a symmetric matrix for all cases.

3 Fundamental analytical solutions of the stress function for anisotropic materials

In the plane problem, the compatibility equation is given by

$$\frac{\partial^2 \varepsilon_x}{\partial y^2}+\frac{\partial^2 \varepsilon_y}{\partial x^2}=\frac{\partial^2 \gamma_{xy}}{\partial x \partial y}. \tag{18}$$

And by introducing the Airy stress function ϕ, the stress components can be written as:

$$\sigma_x=\frac{\partial^2 \phi}{\partial y^2},\quad \sigma_y=\frac{\partial^2 \phi}{\partial x^2},\quad \tau_{xy}=-\frac{\partial^2 \phi}{\partial x \partial y}. \tag{19}$$

Substitution eqs. (6) or (10), and (19) into (18) yields (the symmetry of the reduced elastic compliances $\hat{C}_{ij}$ has been considered):

$$\begin{aligned}\hat{C}_{11}\frac{\partial^4 \phi}{\partial y^4}+\hat{C}_{22}\frac{\partial^4 \phi}{\partial x^4}+\left(2\hat{C}_{12}+\hat{C}_{66}\right)\frac{\partial^4 \phi}{\partial x^2 \partial y^2}\\ -2\hat{C}_{16}\frac{\partial^4 \phi}{\partial x \partial y^3}-2\hat{C}_{26}\frac{\partial^4 \phi}{\partial x^3 \partial y}=0.\end{aligned} \tag{20}$$

Actually, there are numerous polynomials (in global Cartesian coordinates) that can satisfy eq. (20). Here, twenty-three such solutions ϕ_i (i=1–23) and resulting stresses σ_{xi}, σ_{yi} and τ_{xyi} (i=1–23), which have never been reported before in the literature, are listed as follows. There are 3 linearly independent constant stress fields and 4 linearly independent stress fields for each higher degree.

(1) Fundamental solutions of stress function for constant (zero-order) stress fields (i=1–3):

$$\phi_1=x^2 \Rightarrow \begin{cases}\left(\sigma_x\right)_1=0,\\ \left(\sigma_y\right)_1=2,\\ \left(\tau_{xy}\right)_1=0,\end{cases} \tag{21a}$$

$$\phi_2=xy \quad \Rightarrow \begin{cases}\left(\sigma_x\right)_2=0,\\ (\sigma_y)_2=0,\\ \left(\tau_{xy}\right)_2=-1,\end{cases} \tag{21b}$$

$$\phi_3=y^2 \quad \Rightarrow \begin{cases}\left(\sigma_x\right)_3=2,\\ \left(\sigma_y\right)_3=0,\\ \left(\tau_{xy}\right)_3=0.\end{cases} \tag{21c}$$

(2) Fundamental solutions of stress function for linear (first-order) stress fields (i=4–7):

$$\phi_4=x^3 \Rightarrow \begin{cases}\left(\sigma_x\right)_4=0,\\ \left(\sigma_y\right)_4=6x,\\ \left(\tau_{xy}\right)_4=0,\end{cases} \tag{22a}$$

$$\phi_5=x^2 y \Rightarrow \begin{cases}\left(\sigma_x\right)_5=0,\\ \left(\sigma_y\right)_5=2y,\\ \left(\tau_{xy}\right)_5=-2x,\end{cases} \tag{22b}$$

$$\phi_6=xy^2 \Rightarrow \begin{cases}\left(\sigma_x\right)_6=2x,\\ \left(\sigma_y\right)_6=0,\\ \left(\tau_{xy}\right)_6=-2y,\end{cases} \tag{22c}$$

$$\phi_7=y^3 \Rightarrow \begin{cases}\left(\sigma_x\right)_7=6y,\\ \left(\sigma_y\right)_7=0,\\ \left(\tau_{xy}\right)_7=0.\end{cases} \tag{22d}$$

(3) Fundamental solutions of stress function for quadric (second-order) stress fields (i=8–11):

$$\begin{aligned}&\phi_8=\left(2\hat{C}_{12}+\hat{C}_{66}\right)x^4-6\hat{C}_{22}x^2y^2\\ &\Rightarrow\begin{cases}\left(\sigma_x\right)_8=-12\hat{C}_{22}x^2,\\ \left(\sigma_y\right)_8=12\left(2\hat{C}_{12}+\hat{C}_{66}\right)x^2-12\hat{C}_{22}y^2,\\ \left(\tau_{xy}\right)_8=24\hat{C}_{22}xy,\end{cases}\end{aligned} \tag{23a}$$

$$\begin{aligned}&\phi_9=3\hat{C}_{26}x^2y^2+\left(2\hat{C}_{12}+\hat{C}_{66}\right)x^3y^2\\ &\Rightarrow\begin{cases}\left(\sigma_x\right)_9=6\hat{C}_{26}x^2,\\ \left(\sigma_y\right)_9=6\left(2\hat{C}_{12}+\hat{C}_{66}\right)xy+6\hat{C}_{26}y^2,\\ \left(\tau_{xy}\right)_9=-3\left(2\hat{C}_{12}+\hat{C}_{66}\right)x^2-12\hat{C}_{26}xy,\end{cases}\end{aligned} \tag{23b}$$

$$\begin{aligned}&\phi_{10}=3\hat{C}_{16}x^2y^2+\left(2\hat{C}_{12}+\hat{C}_{66}\right)xy^3\\ &\Rightarrow\begin{cases}\left(\sigma_x\right)_{10}=6\hat{C}_{16}x^2+6\left(2\hat{C}_{12}+\hat{C}_{66}\right)xy,\\ \left(\sigma_y\right)_{10}=6\hat{C}_{16}y^2,\\ \left(\tau_{xy}\right)_{10}=-12\hat{C}_{16}xy-3\left(2\hat{C}_{12}+\hat{C}_{66}\right)y^2,\end{cases}\end{aligned} \tag{23c}$$

$$\begin{aligned}&\phi_{11}=-6\hat{C}_{11}x^2y^2+\left(2\hat{C}_{12}+\hat{C}_{66}\right)y^4\\ &\Rightarrow\begin{cases}\left(\sigma_x\right)_{11}=-12\hat{C}_{11}x^2+12(2\hat{C}_{12}+\hat{C}_{66})y^2,\\ \left(\sigma_y\right)_{11}=-12\hat{C}_{11}y^2,\\ \left(\tau_{xy}\right)_{11}=24\hat{C}_{11}xy.\end{cases}\end{aligned} \tag{23d}$$

(4) Fundamental solutions of stress function for cubic (third- order) stress fields (*i*=12–15):

$$\phi_{12}=2\hat{C}_{11}\hat{C}_{26}x^5+5\hat{C}_{11}\hat{C}_{22}x^4y-\hat{C}_{22}^2y^5$$
$$\Rightarrow\begin{cases}(\sigma_x)_{12}=-20\hat{C}_{22}^2y^3,\\(\sigma_y)_{12}=40\hat{C}_{11}\hat{C}_{26}x^3+60\hat{C}_{11}\hat{C}_{22}x^2y,\\(\tau_{xy})_{12}=-20\hat{C}_{11}\hat{C}_{22}x^3,\end{cases}\tag{24a}$$

$$\phi_{13}=-\hat{C}_{11}\left(2\hat{C}_{12}+\hat{C}_{66}\right)x^5+10\hat{C}_{11}\hat{C}_{22}x^3y^2+2\hat{C}_{26}\hat{C}_{22}y^5$$
$$\Rightarrow\begin{cases}(\sigma_x)_{13}=20\hat{C}_{11}\hat{C}_{22}x^3+40\hat{C}_{26}\hat{C}_{22}y^3,\\(\sigma_y)_{13}=-20\hat{C}_{11}(2\hat{C}_{12}+\hat{C}_{66})x^3+60\hat{C}_{11}\hat{C}_{22}xy^2,\\(\tau_{xy})_{13}=-60\hat{C}_{11}\hat{C}_{22}x^2y,\end{cases}\tag{24b}$$

$$\phi_{14}=2\hat{C}_{11}\hat{C}_{16}x^5+10\hat{C}_{11}\hat{C}_{22}x^2y^3-\left(2\hat{C}_{12}+\hat{C}_{66}\right)\hat{C}_{22}y^5$$
$$\Rightarrow\begin{cases}(\sigma_x)_{14}=60\hat{C}_{11}\hat{C}_{22}x^2y-20(2\hat{C}_{12}+\hat{C}_{66})\hat{C}_{22}y^3,\\(\sigma_y)_{14}=40\hat{C}_{11}\hat{C}_{16}x^3+20\hat{C}_{11}\hat{C}_{22}y^3,\\(\tau_{xy})_{14}=-60\hat{C}_{11}\hat{C}_{22}xy^2,\end{cases}\tag{24c}$$

$$\phi_{15}=-\hat{C}_{11}^2x^5+5\hat{C}_{11}\hat{C}_{22}xy^4+2\hat{C}_{22}\hat{C}_{16}y^5$$
$$\Rightarrow\begin{cases}(\sigma_x)_{15}=60\hat{C}_{11}\hat{C}_{22}xy^2+40\hat{C}_{22}\hat{C}_{16}y^3,\\(\sigma_y)_{15}=-20\hat{C}_{11}^2x^3,\\(\tau_{xy})_{15}=-20\hat{C}_{11}\hat{C}_{22}y^3.\end{cases}\tag{24d}$$

(5) Fundamental solutions of stress function for quartic (fourth-order) stress fields (*i*=16–19):

$$\phi_{16}=\hat{C}_{11}\left(\hat{C}_{66}\hat{C}_{26}+2\hat{C}_{12}\hat{C}_{26}-\hat{C}_{22}\hat{C}_{16}\right)x^6-10\hat{C}_{11}\hat{C}_{22}^2x^3y^3+3\hat{C}_{11}\hat{C}_{22}\left(2\hat{C}_{12}+\hat{C}_{66}\right)x^5y-\hat{C}_{22}^2\hat{C}_{26}y^6$$
$$\Rightarrow\begin{cases}(\sigma_x)_{16}=-60\hat{C}_{11}\hat{C}_{22}^2x^3y-30\hat{C}_{22}^2\hat{C}_{26}y^4,\\(\sigma_y)_{16}=30\hat{C}_{11}(\hat{C}_{66}\hat{C}_{26}+2\hat{C}_{12}\hat{C}_{26}-\hat{C}_{22}\hat{C}_{16})x^4-60\hat{C}_{11}\hat{C}_{22}^2xy^3+60\hat{C}_{11}\hat{C}_{22}(2\hat{C}_{12}+\hat{C}_{66})x^3y,\\(\tau_{xy})_{16}=90\hat{C}_{11}\hat{C}_{22}^2x^2y^2-15\hat{C}_{11}\hat{C}_{22}(2\hat{C}_{12}+\hat{C}_{66})x^4,\end{cases}\tag{25a}$$

$$\phi_{17}=-\hat{C}_{11}\left(4\hat{C}_{12}^2+4\hat{C}_{66}\hat{C}_{12}+\hat{C}_{66}^2-4\hat{C}_{16}\hat{C}_{26}\right)x^6+40\hat{C}_{11}\hat{C}_{22}\hat{C}_{26}x^3y^3+15\hat{C}_{11}\hat{C}_{22}\left(2\hat{C}_{12}+\hat{C}_{66}\right)x^4y^2-\hat{C}_{22}\left(2\hat{C}_{22}\hat{C}_{12}+\hat{C}_{22}\hat{C}_{66}-4\hat{C}_{26}^2\right)y^6$$
$$\Rightarrow\begin{cases}(\sigma_x)_{17}=30\hat{C}_{11}\hat{C}_{22}\left(2\hat{C}_{12}+\hat{C}_{66}\right)x^4+240\hat{C}_{11}\hat{C}_{22}\hat{C}_{26}x^3y-30\hat{C}_{22}\left(2\hat{C}_{22}\hat{C}_{12}+\hat{C}_{22}\hat{C}_{66}-4\hat{C}_{26}^2\right)y^4,\\(\sigma_y)_{17}=-30\hat{C}_{11}\left(4\hat{C}_{12}^2+4\hat{C}_{66}\hat{C}_{12}+\hat{C}_{66}^2-4\hat{C}_{16}\hat{C}_{26}\right)x^4+240\hat{C}_{11}\hat{C}_{22}\hat{C}_{26}xy^3+180\hat{C}_{11}\hat{C}_{22}\left(2\hat{C}_{12}+\hat{C}_{66}\right)x^2y^2,\\(\tau_{xy})_{17}=-120\hat{C}_{11}\hat{C}_{22}\left(2\hat{C}_{12}+\hat{C}_{66}\right)x^3y-360\hat{C}_{11}\hat{C}_{22}\hat{C}_{26}x^2y^2,\end{cases}\tag{25b}$$

$$\phi_{18}=-\hat{C}_{11}\left(2\hat{C}_{11}\hat{C}_{12}-4\hat{C}_{16}^2+\hat{C}_{11}\hat{C}_{66}\right)x^6+40\hat{C}_{11}\hat{C}_{22}\hat{C}_{16}x^3y^3+15\hat{C}_{11}\hat{C}_{22}\left(2\hat{C}_{12}+\hat{C}_{66}\right)x^2y^4-\hat{C}_{22}\left(4\hat{C}_{12}^2+4\hat{C}_{66}\hat{C}_{12}+\hat{C}_{66}^2-4\hat{C}_{16}\hat{C}_{26}\right)y^6$$
$$\Rightarrow\begin{cases}(\sigma_x)_{18}=240\hat{C}_{11}\hat{C}_{22}\hat{C}_{16}x^3y+180\hat{C}_{11}\hat{C}_{22}\left(2\hat{C}_{12}+\hat{C}_{66}\right)x^2y^2-30\hat{C}_{22}\left(4\hat{C}_{12}^2+4\hat{C}_{66}\hat{C}_{12}+\hat{C}_{66}^2-4\hat{C}_{16}\hat{C}_{26}\right)y^4,\\(\sigma_y)_{18}=-30\hat{C}_{11}\left(2\hat{C}_{11}\hat{C}_{12}-4\hat{C}_{16}^2+\hat{C}_{11}\hat{C}_{66}\right)x^4+240\hat{C}_{11}\hat{C}_{22}\hat{C}_{16}xy^3+30C_{11}\hat{C}_{22}\left(2\hat{C}_{12}+\hat{C}_{66}\right)y^4,\\(\tau_{xy})_{18}=-360\hat{C}_{11}\hat{C}_{22}\hat{C}_{16}x^2y^2-120\hat{C}_{11}\hat{C}_{22}\left(2\hat{C}_{12}+\hat{C}_{66}\right)xy^3,\end{cases}\tag{25c}$$

$$\phi_{19}=-\hat{C}_{11}^2\hat{C}_{16}x^6-10\hat{C}_{11}^2\hat{C}_{22}x^3y^3+3\hat{C}_{11}\hat{C}_{22}\left(2\hat{C}_{12}+\hat{C}_{66}\right)xy^5+\hat{C}_{22}\left(\hat{C}_{66}\hat{C}_{16}+2\hat{C}_{12}\hat{C}_{16}-\hat{C}_{11}\hat{C}_{26}\right)y^6$$
$$\Rightarrow\begin{cases}(\sigma_x)_{19}=-60\hat{C}_{11}^2\hat{C}_{22}x^3y+60\hat{C}_{11}\hat{C}_{22}\left(2\hat{C}_{12}+\hat{C}_{66}\right)xy^3+30\hat{C}_{22}\left(\hat{C}_{66}\hat{C}_{16}+2\hat{C}_{12}\hat{C}_{16}-\hat{C}_{11}\hat{C}_{26}\right)y^4,\\(\sigma_y)_{19}=-30\hat{C}_{11}^2\hat{C}_{16}x^4-60\hat{C}_{11}^2\hat{C}_{22}xy^3,\\(\tau_{xy})_{19}=90\hat{C}_{11}^2\hat{C}_{22}x^2y^2-15\hat{C}_{11}\hat{C}_{22}(2\hat{C}_{12}+\hat{C}_{66})y^4.\end{cases}\tag{25d}$$

(6) Fundamental solutions of stress function for quintic (fifth-order) stress fields (*i*=20–23):

$$\phi_{20}=-\hat{C}_{11}^2\left(2\hat{C}_{22}\hat{C}_{12}+\hat{C}_{22}\hat{C}_{66}-4\hat{C}_{26}^2\right)x^7+14\hat{C}_{11}^2\hat{C}_{22}\hat{C}_{26}x^6y-7\hat{C}_{11}\hat{C}_{22}^3xy^6+21\hat{C}_{11}^2\hat{C}_{22}^2\hat{C}_{26}x^5y^2-2\hat{C}_{16}\hat{C}_{22}^3y^7$$
$$\Rightarrow\begin{cases}(\sigma_x)_{20}=42\hat{C}_{11}^2\hat{C}_{22}^2x^5-210\hat{C}_{11}\hat{C}_{22}^3xy^4-84\hat{C}_{16}\hat{C}_{22}^3y^5,\\(\sigma_y)_{20}=-42\hat{C}_{11}^2\left(2\hat{C}_{22}\hat{C}_{12}+\hat{C}_{22}\hat{C}_{66}-4\hat{C}_{26}^2\right)x^5+420\hat{C}_{11}^2\hat{C}_{22}\hat{C}_{26}x^4y+420\hat{C}_{11}^2\hat{C}_{22}^2x^3y^2,\\(\tau_{xy})_{20}=-84\hat{C}_{11}^2\hat{C}_{22}\hat{C}_{26}x^5-210\hat{C}_{11}^2\hat{C}_{22}^2x^4y+42\hat{C}_{11}\hat{C}_{22}^3y^5,\end{cases}\tag{26a}$$

$$\phi_{21}=2\hat{C}_{11}^2\left(-2\hat{C}_{12}\hat{C}_{26}+\hat{C}_{22}\hat{C}_{16}-\hat{C}_{66}\hat{C}_{26}\right)x^7-7\hat{C}_{11}^2\hat{C}_{22}\left(2\hat{C}_{12}+\hat{C}_{66}\right)x^6y+14\hat{C}_{11}\hat{C}_{22}^2\hat{C}_{26}xy^6+35\hat{C}_{11}^2\hat{C}_{22}^2x^4y^3-\hat{C}_{22}^2\left(\hat{C}_{11}\hat{C}_{22}-4\hat{C}_{26}\hat{C}_{16}\right)y^7$$

$$\Rightarrow\begin{cases}(\sigma_x)_{21}=210\hat{C}_{11}^2\hat{C}_{22}^2x^4y+420\hat{C}_{11}\hat{C}_{22}^2\hat{C}_{26}xy^4-42\hat{C}_{22}^2\left(\hat{C}_{11}\hat{C}_{22}-4\hat{C}_{26}\hat{C}_{16}\right)y^5,\\(\sigma_y)_{21}=84\hat{C}_{11}^2\left(-2\hat{C}_{12}\hat{C}_{26}+\hat{C}_{22}\hat{C}_{16}-\hat{C}_{66}\hat{C}_{26}\right)x^5-210\hat{C}_{11}^2\hat{C}_{22}\left(2\hat{C}_{12}+\hat{C}_{66}\right)x^4y+420\hat{C}_{11}^2\hat{C}_{22}^2x^2y^3,\\(\tau_{xy})_{21}=42\hat{C}_{11}^2\hat{C}_{22}\left(2\hat{C}_{12}+\hat{C}_{66}\right)x^5-420\hat{C}_{11}^2\hat{C}_{22}^2x^3y^2-84\hat{C}_{11}\hat{C}_{22}^2\hat{C}_{26}y^5,\end{cases}\tag{26b}$$

$$\phi_{22}=-\hat{C}_{11}^2\left(\hat{C}_{11}\hat{C}_{22}-4\hat{C}_{26}\hat{C}_{16}\right)x^7+14\hat{C}_{11}^2\hat{C}_{22}\hat{C}_{16}x^6y-7\hat{C}_{11}\hat{C}_{22}^2\left(2\hat{C}_{12}+\hat{C}_{66}\right)xy^6+35\hat{C}_{11}^2\hat{C}_{22}^2x^3y^4-2\hat{C}_{22}^2\left(2\hat{C}_{12}\hat{C}_{16}-\hat{C}_{11}\hat{C}_{26}+\hat{C}_{66}\hat{C}_{16}\right)y^7$$

$$\Rightarrow\begin{cases}(\sigma_x)_{22}=420\hat{C}_{11}^2\hat{C}_{22}^2\hat{C}_{26}x^3y^2-210\hat{C}_{11}\hat{C}_{22}^2\left(2\hat{C}_{12}+\hat{C}_{66}\right)xy^4-84\hat{C}_{22}^2\left(2\hat{C}_{12}\hat{C}_{16}-\hat{C}_{11}\hat{C}_{26}+\hat{C}_{66}\hat{C}_{16}\right)y^5,\\(\sigma_y)_{22}=-42\hat{C}_{11}^2\left(\hat{C}_{11}\hat{C}_{22}-4\hat{C}_{26}\hat{C}_{16}\right)x^5+420\hat{C}_{11}^2\hat{C}_{22}\hat{C}_{16}x^4y+210\hat{C}_{11}^2\hat{C}_{22}^2xy^4,\\(\tau_{xy})_{22}=-84\hat{C}_{11}^2\hat{C}_{22}\hat{C}_{16}x^5-420\hat{C}_{11}^2\hat{C}_{22}^2x^2y^3+42\hat{C}_{11}\hat{C}_{22}^2\left(2\hat{C}_{12}+\hat{C}_{66}\right)y^5,\end{cases}\tag{26c}$$

$$\phi_{23}=-2\hat{C}_{11}^3\hat{C}_{26}x^7-7\hat{C}_{11}^3\hat{C}_{22}x^6y+14\hat{C}_{11}\hat{C}_{22}^2\hat{C}_{16}xy^6+21\hat{C}_{11}^2\hat{C}_{22}^2\hat{C}_{26}x^2y^5-\hat{C}_{22}^2\left(2\hat{C}_{11}\hat{C}_{12}+\hat{C}_{11}\hat{C}_{66}-4\hat{C}_{16}^2\right)y^7$$

$$\Rightarrow\begin{cases}(\sigma_x)_{23}=420\hat{C}_{11}\hat{C}_{22}^2\hat{C}_{16}xy^4+420\hat{C}_{11}^2\hat{C}_{22}^2x^2y^3-42\hat{C}_{22}^2\left(2\hat{C}_{11}\hat{C}_{12}+\hat{C}_{11}\hat{C}_{66}-4\hat{C}_{16}^2\right)y^5,\\(\sigma_y)_{23}=-84\hat{C}_{11}^3\hat{C}_{26}x^5-210\hat{C}_{11}^3\hat{C}_{22}x^4y+42\hat{C}_{11}^2\hat{C}_{22}^2y^5,\\(\tau_{xy})_{23}=42\hat{C}_{11}^3\hat{C}_{22}x^5-210\hat{C}_{11}^2\hat{C}_{22}^2xy^4-84\hat{C}_{11}\hat{C}_{22}^2\hat{C}_{16}y^5.\end{cases}\tag{26d}$$

In order to choose appropriate solutions as the trial functions for the construction of a new element model, two principles must be followed: (i) the fundamental analytical solutions ϕ_i of the stress function ϕ should be selected in turn from the lowest-order to a higher-order; and (ii) the resulting stress fields should possess completeness in Cartesian coordinates.

4 The formulations of 8- and 12-node plane hybrid stress-function elements for anisotropic materials

As shown in Figure 2, (ξ, η) are the isoparametric coordinates. The shapes of the 8- and 12-node plane quadrilateral elements can be both convex and concave. The complementary energy functional of a plane finite element model can be written in the following matrix form [31]:

$$\Pi_C=\Pi_C^*+V_C^*=\frac{1}{2}\iint_{A^e}\boldsymbol{\sigma}^{\mathrm{T}}\boldsymbol{C}\boldsymbol{\sigma}t\mathrm{d}A-\int_{\Gamma^e}\boldsymbol{T}^{\mathrm{T}}\overline{\boldsymbol{u}}t\mathrm{d}s,\tag{27}$$

with

$$\Pi_C^*=\frac{1}{2}\iint_{A^e}\boldsymbol{\sigma}^{\mathrm{T}}\boldsymbol{C}\boldsymbol{\sigma}t\mathrm{d}A,\quad V_C^*=-\int_{\Gamma^e}\boldsymbol{T}^{\mathrm{T}}\overline{\boldsymbol{u}}t\mathrm{d}s,\tag{28}$$

$$\boldsymbol{\sigma}=\begin{Bmatrix}\sigma_x\\\sigma_y\\\tau_{xy}\end{Bmatrix},\quad\boldsymbol{T}=\begin{Bmatrix}T_x\\T_y\end{Bmatrix},\quad\overline{\boldsymbol{u}}=\begin{Bmatrix}\overline{u}\\\overline{v}\end{Bmatrix},\tag{29}$$

where Π_C^* is the complementary energy within the element;

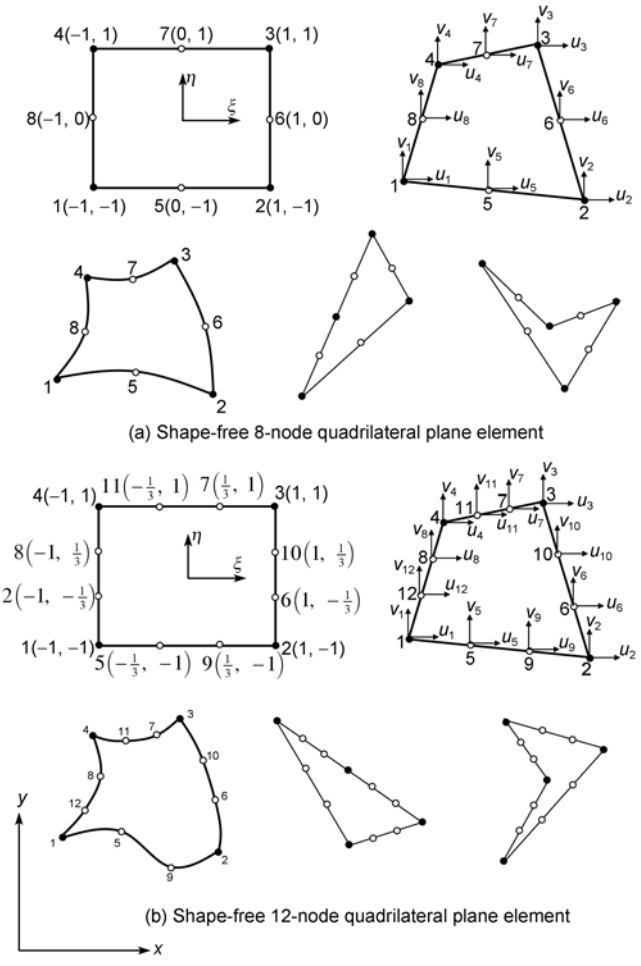

Figure 2 8- and 12-node shape-free quadrilateral plane element.

V_C^* is the complementary energy along the kinematic boundaries (here, all element boundaries are treated as the kinematic boundaries because the boundary displacements will be prescribed in eq. (30)); t is the thickness of the element; $\boldsymbol{C}$ is the elasticity matrix of compliances and has been given in sect. 2; $\boldsymbol{\sigma}$ is the element stress vector; $\boldsymbol{T}$ is the traction force vector along the element boundaries; $\overline{\boldsymbol{u}}$ is the displacement vector along element boundaries, which can be interpolated by the element nodal displacement vector $\boldsymbol{q}^e$:

$$\overline{\boldsymbol{u}} = \overline{\boldsymbol{N}}\big|_{\Gamma}\,\boldsymbol{q}^e, \tag{30}$$

with

$$\boldsymbol{q}^e = [u_1 \quad v_1 \quad u_2 \quad v_2 \quad \cdots \quad \cdots \quad u_I \quad v_I]^{\mathrm{T}}, \tag{31}$$

$$\overline{\boldsymbol{N}} = \begin{bmatrix} N_1^0 & 0 & N_2^0 & 0 & \cdots & \cdots & N_I^0 & 0 \\ 0 & N_1^0 & 0 & N_2^0 & \cdots & \cdots & 0 & N_I^0 \end{bmatrix}, \tag{32}$$

For 8-node elements, I=8, and

$$N_i^0 = \begin{cases} -\dfrac{1}{4}(1+\xi_i\xi)(1+\eta_i\eta)(1-\xi_i\xi-\eta_i\eta), & (i=1,2,3,4), \\ \dfrac{1}{2}(1-\xi^2)(1+\eta_i\eta), & (i=5,7), \\ \dfrac{1}{2}(1-\eta^2)(1+\xi_i\xi), & (i=6,8), \end{cases} \tag{33}$$

where (ξ_i, η_i) are the isoparametric coordinates of node i. For 12-node elements, I=12, and

$$N_i^0 = \begin{cases} -\dfrac{1}{32}(1+\xi_i\xi)(1+\eta_i\eta)(10-9\xi^2-9\eta^2), & (i=1,2,3,4), \\ \dfrac{9}{32}(1-\xi^2)\left(1+\dfrac{\xi}{\xi_i}\right)(1+\eta_i\eta), & (i=5,7,9,11), \\ \dfrac{9}{32}(1-\eta^2)\left(1+\dfrac{\eta}{\eta_i}\right)(1+\xi_i\xi), & (i=6,8,10,12). \end{cases} \tag{34}$$

Therefore, the displacements along the element edges, $\overline{12}$ ($\eta=-1$), $\overline{23}$ ($\xi=1$), $\overline{34}$ ($\eta=1$) and $\overline{41}$ ($\xi=-1$), can be given as follows:

$$\begin{aligned} \overline{\boldsymbol{u}}_{\overline{12}} &= \begin{Bmatrix} \overline{u} \\ \overline{v} \end{Bmatrix}_{\overline{12}} = \overline{\boldsymbol{N}}\big|_{\eta=-1}\,\boldsymbol{q}^e, \quad \overline{\boldsymbol{u}}_{\overline{23}} = \begin{Bmatrix} \overline{u} \\ \overline{v} \end{Bmatrix}_{\overline{23}} = \overline{\boldsymbol{N}}\big|_{\xi=1}\,\boldsymbol{q}^e, \\ \overline{\boldsymbol{u}}_{\overline{34}} &= \begin{Bmatrix} \overline{u} \\ \overline{v} \end{Bmatrix}_{\overline{34}} = \overline{\boldsymbol{N}}\big|_{\eta=1}\,\boldsymbol{q}^e, \quad \overline{\boldsymbol{u}}_{\overline{41}} = \begin{Bmatrix} \overline{u} \\ \overline{v} \end{Bmatrix}_{\overline{41}} = \overline{\boldsymbol{N}}\big|_{\xi=-1}\,\boldsymbol{q}^e. \end{aligned} \tag{35}$$

With the introduction of the Airy stress function ϕ, the stress vector $\boldsymbol{\sigma}$ can be expressed by

$$\boldsymbol{\sigma} = \begin{Bmatrix} \sigma_x \\ \sigma_y \\ \tau_{xy} \end{Bmatrix} = \begin{Bmatrix} \dfrac{\partial^2\phi}{\partial y^2} \\ \dfrac{\partial^2\phi}{\partial x^2} \\ -\dfrac{\partial^2\phi}{\partial x\partial y} \end{Bmatrix} = \tilde{\boldsymbol{R}}(\phi), \tag{36}$$

and the traction force vector $\boldsymbol{T}$ can be written as:

$$\boldsymbol{T} = \begin{Bmatrix} T_x \\ T_y \end{Bmatrix} = \begin{bmatrix} l & 0 & m \\ 0 & m & l \end{bmatrix} \begin{Bmatrix} \sigma_x \\ \sigma_y \\ \tau_{xy} \end{Bmatrix} = \boldsymbol{L}\tilde{\boldsymbol{R}}(\phi), \tag{37}$$

where l and m are the direction cosines of the outer normal $\boldsymbol{n}$ of the element boundaries.

Substitution of eqs. (36) and (37) into eq. (27) yields

$$\begin{aligned} \Pi_C &= \Pi_C^* + V_C^* \\ &= \frac{1}{2}\iint_{A^e} \tilde{\boldsymbol{R}}(\phi)^{\mathrm{T}}\boldsymbol{C}\tilde{\boldsymbol{R}}(\phi)t\mathrm{d}A - \int_{\Gamma}\left[\boldsymbol{L}\tilde{\boldsymbol{R}}(\phi)\right]^{\mathrm{T}}\overline{\boldsymbol{u}}t\mathrm{d}s, \end{aligned} \tag{38}$$

where

$$\Pi_C^* = \frac{1}{2}\iint_{A^e} \tilde{\boldsymbol{R}}(\phi)^{\mathrm{T}}\boldsymbol{C}\tilde{\boldsymbol{R}}(\phi)t\mathrm{d}A,\ V_C^* = -\int_{\Gamma}\left[\boldsymbol{L}\tilde{\boldsymbol{R}}(\phi)\right]^{\mathrm{T}}\overline{\boldsymbol{u}}t\mathrm{d}s. \tag{39}$$

Let

$$\phi = \sum_{i=1}^{J}\phi_i\beta_i = \boldsymbol{\varphi}\boldsymbol{\beta}, \tag{40}$$

with

$$\begin{aligned} \boldsymbol{\varphi} &= [\phi_1 \quad \phi_2 \quad \phi_3 \quad \cdots \quad \cdots \quad \phi_J], \\ \boldsymbol{\beta} &= [\beta_1 \quad \beta_2 \quad \beta_3 \quad \cdots \quad \cdots \quad \beta_J]^{\mathrm{T}}, \end{aligned} \tag{41}$$

where J is the number of the fundamental analytical solutions used for stress function ϕ in eq. (40); ϕ_i (i=1–J) are J fundamental analytical solutions (in Cartesian coordinates) of the Airy stress function ϕ, which must be selected from complete second-order terms (x^2, y^2, xy) to complete higher-order terms (see eqs. (21) to (26) in sect. 3), and satisfy the compatibility eq. (20); β_i (i=1–J) are J unknown constants. Obviously, such trial functions will directly lead to more reasonable stress fields satisfying both equilibrium and compatibility conditions.

Substitution of eq. (40) into the first expression of eq. (39) yields

$$\Pi_C^* = \frac{1}{2}\boldsymbol{\beta}^{\mathrm{T}}\boldsymbol{M}\boldsymbol{\beta}, \tag{42}$$

with

$$\boldsymbol{M} = \iint_{A^e} \boldsymbol{S}^{\mathrm{T}}\boldsymbol{C}\boldsymbol{S}t\mathrm{d}A, \tag{43}$$

in which $\boldsymbol{S}$ is the stress solution matrix, and

$$\boldsymbol{S} = \begin{bmatrix} (\sigma_x)_1 & (\sigma_x)_2 & (\sigma_x)_3 & \cdots & (\sigma_x)_J \\ (\sigma_y)_1 & (\sigma_y)_2 & (\sigma_y)_3 & \cdots & (\sigma_y)_J \\ (\tau_{xy})_1 & (\tau_{xy})_2 & (\tau_{xy})_3 & \cdots & (\tau_{xy})_J \end{bmatrix}, \tag{44}$$

where $(\sigma_x)_i$, $(\sigma_y)_i$ and $(\tau_{xy})_i$ (i=1–J) are given by eqs. (21) to (26). For 8-node elements, let J=15, and the resulting model is denoted by SF8(15$\boldsymbol{\beta}$); and for 12-node elements, let J=23, the resulting model is denoted by SF12(23$\boldsymbol{\beta}$). $\boldsymbol{M}$ is the flexibility matrix, and its evaluation procedure has been given in ref. [31].

And substitution of eqs. (30) and (40) into the second expression of eq. (39) yields

$$V_C^* = -\boldsymbol{\beta}^{\mathrm{T}}\boldsymbol{H}\boldsymbol{q}^e, \tag{45}$$

with

$$\boldsymbol{H} = \int_\Gamma \boldsymbol{S}^{\mathrm{T}}\boldsymbol{L}^{\mathrm{T}}\bar{\boldsymbol{N}}t\mathrm{d}s, \tag{46}$$

where $\boldsymbol{H}$ is the leverage matrix, and its evaluation procedure has also been given in ref. [31].

Then, after substituting eqs. (42) and (45) into eq. (38), the element complementary energy functional can be re-written as:

$$\Pi_C = \frac{1}{2}\boldsymbol{\beta}^{\mathrm{T}}\boldsymbol{M}\boldsymbol{\beta} - \boldsymbol{\beta}^{\mathrm{T}}\boldsymbol{H}\boldsymbol{q}^e. \tag{47}$$

According to the principle of minimum complementary energy, we have

$$\frac{\partial \Pi_C}{\partial \boldsymbol{\beta}} = \boldsymbol{0}. \tag{48}$$

Thus, by substituting eq. (48) into eq. (47), the unknown constant vector $\boldsymbol{\beta}$ can be expressed in terms of the nodal displacement vector $\boldsymbol{q}^e$:

$$\boldsymbol{\beta} = \boldsymbol{M}^{-1}\boldsymbol{H}\boldsymbol{q}^e. \tag{49}$$

Substitution of eq. (49) into eq. (42) yields

$$\Pi_C^* = \frac{1}{2}\boldsymbol{q}^{e\mathrm{T}}\boldsymbol{K}^*\boldsymbol{q}^e, \tag{50}$$

where

$$\boldsymbol{K}^* = \left(\boldsymbol{M}^{-1}\boldsymbol{H}\right)^{\mathrm{T}}\boldsymbol{H} = \boldsymbol{H}^{\mathrm{T}}\boldsymbol{M}^{-1}\boldsymbol{H}. \tag{51}$$

From the viewpoint of the hybrid stress element [30], matrix $\boldsymbol{K}^*$ in the above equation can be considered as the stiffness matrix of the hybrid stress-function element, and therefore, it can readily be incorporated into the standard finite element program framework.

Once the element nodal displacement vector $\boldsymbol{q}^e$ is solved, the element stresses can be given by

$$\boldsymbol{\sigma} = \boldsymbol{S}\boldsymbol{M}^{-1}\boldsymbol{H}\boldsymbol{q}^e. \tag{52}$$

The stress solutions at any point can be readily obtained by substituting the Cartesian coordinates of this point within an element into $\boldsymbol{S}$ in the above equation, and then, the resulting strains can be obtained by constitutive equations.

The determination procedure of the nodal equivalent load vector $\boldsymbol{R}^e$ is the same as that of the conventional displacement-based isoparametric elements:

$$\boldsymbol{R}^e = \iint_{A^e} \bar{\boldsymbol{N}}^{\mathrm{T}}\boldsymbol{f}^e\mathrm{d}A \quad \text{with} \quad \boldsymbol{f}^e = \begin{bmatrix} f_x & f_y \end{bmatrix}^{\mathrm{T}}, \tag{53}$$

$$\boldsymbol{R}^e = \int_{\Gamma^e} \bar{\boldsymbol{N}}\big|_\Gamma^{\mathrm{T}}\boldsymbol{p}^e\mathrm{d}\Gamma \quad \text{with} \quad \boldsymbol{p}^e = \begin{bmatrix} p_x & p_y \end{bmatrix}^{\mathrm{T}}, \tag{54}$$

where $\boldsymbol{f}^e$ and $\boldsymbol{p}^e$ are the element body force and boundary distributed load vectors, respectively.

5 Numerical examples

5.1 Patch Tests for constant, linear and quadric strain/stress problems (Figure 3)

As shown in Figure 3, a small anisotropic plane stress patch (the thickness t=1) is meshed by five elements with severely distorted shapes, in which some elements are even concave. It should be noted that usual isoparametric finite elements cannot work using such a severely distorted mesh. The material constants are given by

$$\begin{bmatrix} D_{11} & D_{12} & D_{13} & D_{16} \\ D_{21} & D_{22} & D_{23} & D_{26} \\ D_{31} & D_{32} & D_{33} & D_{36} \\ D_{61} & D_{62} & D_{63} & D_{66} \end{bmatrix} = \begin{bmatrix} 2 & 0.8 & 0.5 & 0.5 \\ & 1.5 & 0.5 & 0.4 \\ & \text{sym.} & 1 & 0.5 \\ & & & 1 \end{bmatrix} \times 10^6. \tag{55}$$

Thus, according to eqs. (3–5), the reduced elastic moduli matrix can be written as

$$\begin{bmatrix} \hat{D}_{11} & \hat{D}_{12} & \hat{D}_{16} \\ \hat{D}_{21} & \hat{D}_{22} & \hat{D}_{26} \\ \hat{D}_{61} & \hat{D}_{62} & \hat{D}_{66} \end{bmatrix} = \begin{bmatrix} 1.75 & 0.55 & 0.25 \\ 0.55 & 1.25 & 0.15 \\ 0.25 & 0.15 & 0.75 \end{bmatrix} \times 10^6, \tag{56}$$

and the elasticity matrix of compliances is given by

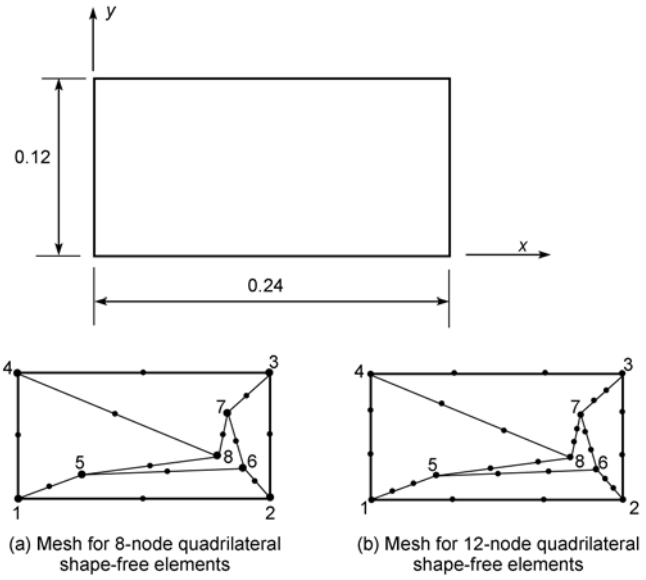

(a) Mesh for 8-node quadrilateral shape-free elements

(b) Mesh for 12-node quadrilateral shape-free elements

Figure 3 Constant, linear and quadric stress/strain patch test.

$$\boldsymbol{C}=\begin{bmatrix}\hat{C}_{11} & \hat{C}_{12} & \hat{C}_{16}\\ \hat{C}_{21} & \hat{C}_{22} & \hat{C}_{26}\\ \hat{C}_{61} & \hat{C}_{62} & \hat{C}_{66}\end{bmatrix}=\begin{bmatrix}\hat{D}_{11} & \hat{D}_{12} & \hat{D}_{16}\\ \hat{D}_{21} & \hat{D}_{22} & \hat{D}_{26}\\ \hat{D}_{61} & \hat{D}_{62} & \hat{D}_{66}\end{bmatrix}^{-1}$$
$$=\begin{bmatrix}0.6841121495 & -0.2803738318 & -0.1719626168\\ -0.2803738318 & 0.9345794393 & -0.0934579439\\ -0.1719626168 & -0.0934579439 & 1.4093457944\end{bmatrix}\times 10^{-6} \tag{57}$$

(1) Constant strain/stress problem. One of the displacement fields corresponding to the constant strain is

$$\begin{aligned}u&=10^3\left[\left(2\hat{C}_{11}+2\hat{C}_{12}-\hat{C}_{16}\right)x+\left(\hat{C}_{16}+\hat{C}_{26}-\frac{1}{2}\hat{C}_{66}\right)y\right]\\ v&=10^3\left[\left(\hat{C}_{16}+\hat{C}_{26}-\frac{1}{2}\hat{C}_{66}\right)x+\left(2\hat{C}_{22}+2\hat{C}_{12}-\hat{C}_{26}\right)y\right]\end{aligned}. \tag{58}$$

The exact stress solutions are as follows:

$$\sigma_x=2000,\quad \sigma_y=2000,\quad \tau_{xy}=-1000. \tag{59}$$

The coordinates of control nodes are shown in Table 1. And the displacements of all boundary nodes are the displacement boundary conditions.

The numerical solutions of displacements and stresses at selected nodes are given in Table 1. It can be seen that the exact results of the displacements and stresses at each node can be obtained using the present 8-node and 12-node elements.

(2) Linear strain/stress problem. One of the displacement fields corresponding to the linear strain is:

$$\begin{aligned}u&=10^3\left[\left(\hat{C}_{11}-\hat{C}_{16}\right)x^2+2\left(\hat{C}_{12}-\hat{C}_{16}\right)xy\right.\\ &\quad\left.+\left(2\hat{C}_{26}-\hat{C}_{12}-\hat{C}_{66}\right)y^2\right]\\ v&=10^3\left[\left(2\hat{C}_{16}-\hat{C}_{12}-\hat{C}_{66}\right)x^2+2\left(\hat{C}_{12}-\hat{C}_{26}\right)xy\right.\\ &\quad\left.+\left(\hat{C}_{22}-\hat{C}_{26}\right)x^2\right].\end{aligned} \tag{60}$$

The exact stress solution is as follows:

$$\sigma_x=2x\times 10^3,\quad \sigma_y=2y\times 10^3,\quad \tau_{xy}=-2(x+y)\times 10^3. \tag{61}$$

The displacements of all boundary nodes are the displacement boundary conditions. From Table 2, it can be seen again that the exact results of the displacements and stresses at each node can be obtained using the present elements SF8(15β) and SF12(23β).

Table 1 Results at selected nodes for the constant stress/strain patch test

Node no.	Coordinates			Results				
	x	y		$u\times10^4$	$v\times10^4$	σ_x	σ_y	τ_{xy}
1	0.0	0.0	SF8(15β)	0.0 (BC)	0.0 (BC)	2000.00	2000.00	−1000.00
			SF12(23β)			2000.00	2000.00	−1000.00
			Exact			2000	2000	−1000
2	0.24	0.0	SF8(15β)	2.35065 (BC)	−2.32822 (BC)	2000.00	2000.00	−1000.00
			SF12(23β)			2000.00	2000.00	−1000.00
			Exact			2000	2000	−1000
3	0.24	0.12	SF8(15β)	1.18654 (BC)	−0.645981 (BC)	2000.00	2000.00	−1000.00
			SF12(23β)			2000.00	2000.00	−1000.00
			Exact			2000	2000	−1000
4	0.0	0.12	SF8(15β)	−1.16411 (BC)	1.68224 (BC)	2000.00	2000.00	−1000.00
			SF12(23β)			2000.00	2000.00	−1000.00
			Exact			2000	2000	−1000
5	0.06	0.02	SF8(15β)	0.393645	−0.301682	2000.00	2000.00	−1000.00
			SF12(23β)	0.393645	−0.301682	2000.00	2000.00	−1000.00
			Exact	0.393645	−0.301682	2000	2000	−1000
6	0.22	0.03	SF8(15β)	1.86374	−1.71364	2000.00	2000.00	−1000.00
			SF12(23β)	1.86374	−1.71364	2000.00	2000.00	−1000.00
			Exact	1.86374	−1.71364	2000	2000	−1000
7	0.2	0.08	SF8(15β)	1.18280	−0.818692	2000.00	2000.00	−1000.00
			SF12(23β)	1.18280	−0.818692	2000.00	2000.00	−1000.00
			Exact	1.18280	−0.818692	2000	2000	−1000
8	0.19	0.04	SF8(15β)	1.47290	−1.28243	2000.00	2000.00	−1000.00
			SF12(23β)	1.47290	−1.28243	2000.00	2000.00	−1000.00
			Exact	1.47290	−1.28243	2000	2000	−1000

Table 2 Results at selected nodes for the linear stress/strain patch test

Node no.	Coordinates			Results				
	x	y		$u\times10^4$	$v\times10^4$	σ_x	σ_y	τ_{xy}
1	0.0	0.0	SF8(15β)	0.0 (BC)	0.0 (BC)	0.000	0.000	0.000
			SF12(23β)			–0.000	0.000	0.000
			Exact			0	0	0
2	0.24	0.0	SF8(15β)	4.93099 (BC)	–8.48389 (BC)	480.000	–0.000	–480.000
			SF12(23β)			480.000	–0.002	–480.000
			Exact			480	0	–480
3	0.24	0.12	SF8(15β)	2.41166 (BC)	–8.08015 (BC)	480.000	240.000	–720.000
			SF12(23β)			480.000	240.000	–720.000
			Exact			480	240	–720
4	0.0	0.12	SF8(15β)	–1.89488 (BC)	1.48037 (BC)	–0.000	240.000	–240.000
			SF12(23β)			0.000	240.000	–240.000
			Exact			0	240	–240
5	0.06	0.02	SF8(15β)	0.22953	–0.53398	120.000	40.0000	–160.000
			SF12(23β)	0.22953	–0.53398	120.000	40.0000	–160.000
			Exact	0.22953	–0.53398	120	40	–160
6	0.22	0.03	SF8(15β)	3.88187	–7.28303	440.000	60.0000	–500.000
			SF12(23β)	3.88187	–7.28303	440.000	60.0000	–500.000
			Exact	3.88187	–7.28303	440	60	–500
7	0.2	0.08	SF8(15β)	2.23521	–5.83178	400.000	160.000	–560.000
			SF12(23β)	2.23521	–5.83178	400.000	160.000	–560.000
			Exact	2.23521	–5.83178	400	160	–560
8	0.19	0.04	SF8(15β)	2.71510	–5.43679	380.000	80.0000	–460.000
			SF12(23β)	2.71510	–5.43679	380.000	80.0000	–460.000
			Exact	2.71510	–5.43679	380	80	–460

(3) Linear strain/stress problem. One of the displacement fields corresponding to the quadric strain can be written as:

$$\begin{aligned} u &= 10^3\left(-4\hat{C}_{11}\hat{C}_{12}x^3+12\hat{C}_{11}\hat{C}_{22}xy^2+4\hat{C}_{22}\hat{C}_{16}y^3\right)\\ v &= 10^3\left(-4\hat{C}_{11}\hat{C}_{26}x^3-12\hat{C}_{11}\hat{C}_{22}x^2y+4\hat{C}_{22}\hat{C}_{12}y^3\right). \end{aligned} \tag{62}$$

The exact stress solution is as follows:

$$\sigma_x = 12\hat{C}_{22}y^2\times10^3,\quad \sigma_y = -12\hat{C}_{11}x^2\times10^3,\quad \tau_{xy}=0. \tag{63}$$

This test is only implemented for 12-node element SF12(23β). Again, the displacements of all boundary nodes are the displacement boundary conditions. The numerical results listed in Table 3 show that element SF12(23β) can produce the exact results for both displacements and stresses in this test.

5.2 A triangular orthotropic patch subjected to linearly distributed loads

As shown in Figure 4, a triangular orthotropic plane stress patch (the thickness t=1) is subjected to three linearly distributed loads. Two mesh divisions are employed here: (a) one triangular degenerated quadrilateral element, which cannot be used by usual quadrilateral isoparametric elements; and (b) three distorted quadrilateral elements. The material constants are given by

$$\begin{aligned} &E_{x'}=135\times10^9;\quad E_{y'}=8.8\times10^9;\\ &\mu_{y'x'}=0.33;\qquad G_{x'y'}=4.47\times10^9. \end{aligned} \tag{64}$$

And three angle cases between the material and global axes are considered: θ=0°, 45°, and 90°. Thus, the corresponding elasticity matrices of compliances, $\boldsymbol{C}$, can be obtained through eqs. (13) to (16).

The exact stress solutions should be as follows:

$$\sigma_x = y,\quad \sigma_y = -2x-y,\quad \tau_{xy}=x. \tag{65}$$

The numerical results at selected points obtained by the present elements SF8(15β) and SF12(23β) are given in Table 4. It can be seen that both elements can produce the exact results for all cases, while the usual isoparametric elements cannot achieve.

Table 3 Results at selected nodes for the quadric stress/strain patch test

Node no.	Coordinates			Results				
	x	y		$u\times10^{11}$	$v\times10^{11}$	$\sigma_x\times10^4$	$\sigma_y\times10^4$	$\tau_{xy}\times10^4$
1	0.0	0.0	SF12(23β)	0.0	0.0	0.0000	0.0000	0.0000
			Exact	(BC)	(BC)	0	0	0
2	0.24	0.0	SF12(23β)	1.06062	0.353539	0.0000	–4.7286	0.0000
			Exact	(BC)	(BC)	0	–4.7286	0
3	0.24	0.12	SF12(23β)	3.60107	–5.13066	1.6149	–4.7286	0.0000
			Exact	(BC)	(BC)	1.6150	–4.7286	0
4	0.0	0.12	SF12(23β)	–0.111085	–0.181116	1.6150	0.0000	0.0000
			Exact	(BC)	(BC)	1.6150	0	0
5	0.06	0.02	SF12(23β)	0.03447	–0.05056	0.04486	–0.29553	0.0000
			Exact	0.03447	–0.05056	0.04486	–0.29554	0
6	0.22	0.03	SF12(23β)	0.96712	–0.84453	0.10094	–3.9733	0.0000
			Exact	0.96712	–0.84453	0.10093	–3.9733	0
7	0.2	0.08	SF12(23β)	1.56292	–2.30420	0.71776	–3.2837	0.0000
			Exact	1.56292	–2.30420	0.71776	–3.2837	0
8	0.19	0.04	SF12(23β)	0.75537	–0.93917	0.17944	–2.9636	0.0000
			Exact	0.75537	–0.93917	0.17944	–2.9636	0

Table 4 Results at selected points for a triangular orthotropic patch subjected to linearly distributed loads

(a) $\theta = 0°$

			Q8	Q12	SF8(15β)	SF12(23β)	Exact
	$\sigma_x(0,-1)$		—	—	–1.0000	–1.0000	–1.0
	$\sigma_y(0,-1)$		—	—	1.0000	1.0000	1.0
	$\tau_{xy}(0,-1)$		—	—	–0.0000	0.0000	0.0
Mesh (a)	$\sigma_x(0.5,-0.5)$		—	—	–0.5000	–0.5000	–0.5
	$\sigma_y(0.5,-0.5)$		—	—	–0.5000	–0.5000	–0.5
	$\tau_{xy}(0.5,-0.5)$		—	—	0.5000	0.5000	0.5
	$u(0,0)\times10^{10}$		—	—	2.2057	2.2057	2.2057
Mesh (b)	$\sigma_x(0.3,-0.7)$	Element ①	–0.6872	–0.6755	–0.7000	–0.7000	–0.7
		Element ②	–1.5057	–1.2719	–0.7000	–0.7000	
		Element ③	–0.2881	–0.3964	–0.7000	–0.7000	
	$\sigma_y(0.3,-0.7)$	Element ①	0.1405	0.1519	0.1000	0.1000	0.1
		Element ②	0.0863	0.0700	0.1000	0.1000	
		Element ③	0.1369	0.1349	0.1000	0.1000	
	$\tau_{xy}(0.3,-0.7)$	Element ①	0.3314	0.3370	0.3000	0.3000	0.3
		Element ②	0.2792	0.2854	0.3000	0.3000	
		Element ③	0.3243	0.3393	0.3000	0.3000	
	$u(0,0)\times10^{10}$		2.16040	2.15958	2.2057	2.2057	2.2057

(b) $\theta = 45°$

			Q8	Q12	SF8(15β)	SF12(23β)	Exact
	$\sigma_x(0,-1)$		—	—	–1.0000	–1.0000	–1.0
	$\sigma_y(0,-1)$		—	—	1.0000	1.0000	1.0
	$\tau_{xy}(0,-1)$		—	—	–0.0000	0.0000	0.0
Mesh (a)	$\sigma_x(0.5,-0.5)$		—	—	–0.5000	–0.5000	–0.5
	$\sigma_y(0.5,-0.5)$		—	—	–0.5000	–0.5000	–0.5
	$\tau_{xy}(0.5,-0.5)$		—	—	0.5000	0.5000	0.5
	$U(0,0)\times10^{10}$		—	—	1.7168	1.7168	1.7168
	$\sigma_x(0.3,-0.7)$	Element ①	–0.5174	–0.5073	–0.7000	–0.7000	–0.7
		Element ②	–0.9124	–0.7832	–0.7000	–0.7000	
		Element ③	–0.4993	–0.4989	–0.7000	–0.7000	
	$\sigma_y(0.3,-0.7)$	Element ①	0.3254	0.3464	0.1000	0.1000	0.1
		Element ②	–0.0489	0.0683	0.1000	0.1000	
Mesh (b)		Element ③	0.3235	0.3406	0.1000	0.1000	
	$\tau_{xy}(0.3,-0.7)$	Element ①	0.1311	0.5102	0.3000	0.3000	0.3
		Element ②	0.2792	0.2439	0.3000	0.3000	
		Element ③	0.5014	0.5096	0.3000	0.3000	
	$u(0,0)\times10^{10}$		1.6457	1.6588	1.7168	1.7168	1.7168

(*To be continued on the next page*)

(c) $\theta = 90°$ (*Continued*)

			Q8	Q12	SF8(15β)	SF12(23β)	Exact
	$\sigma_x(0, -1)$		—	—	−1.0000	−1.0000	−1.0
	$\sigma_y(0, -1)$		—	—	1.0000	1.0000	1.0
	$\tau_{xy}(0, -1)$		—	—	−0.0000	0.0000	0.0
Mesh (a)	$\sigma_x(0.5, -0.5)$		—	—	−0.5000	−0.5000	−0.5
	$\sigma_y(0.5, -0.5)$		—	—	−0.5000	−0.5000	−0.5
	$\tau_{xy}(0.5, -0.5)$		—	—	0.5000	0.5000	0.5
	$u(0,0)\times10^{10}$		—	—	0.6122	0.6122	0.6122
Mesh (b)	$\sigma_x(0.3, -0.7)$	Element ①	−0.7098	−0.7135	−0.7000	−0.7000	−0.7
		Element ②	−0.7225	−0.7052	−0.7000	−0.7000	
		Element ③	−0.7139	−0.7227	−0.7000	−0.7000	
	$\sigma_y(0.3, -0.7)$	Element ①	0.3188	0.2264	0.1000	0.1000	0.1
		Element ②	−0.2601	−0.0452	0.1000	0.1000	
		Element ③	0.1259	0.1319	0.1000	0.1000	
	$\tau_{xy}(0.3, -0.7)$	Element ①	0.2949	0.2969	0.3000	0.3000	0.3
		Element ②	0.2820	0.3017	0.3000	0.3000	
		Element ③	0.3011	0.3036	0.3000	0.3000	
	$u(0,0)\times10^{10}$		0.6027	0.6068	0.6122	0.6122	0.6122

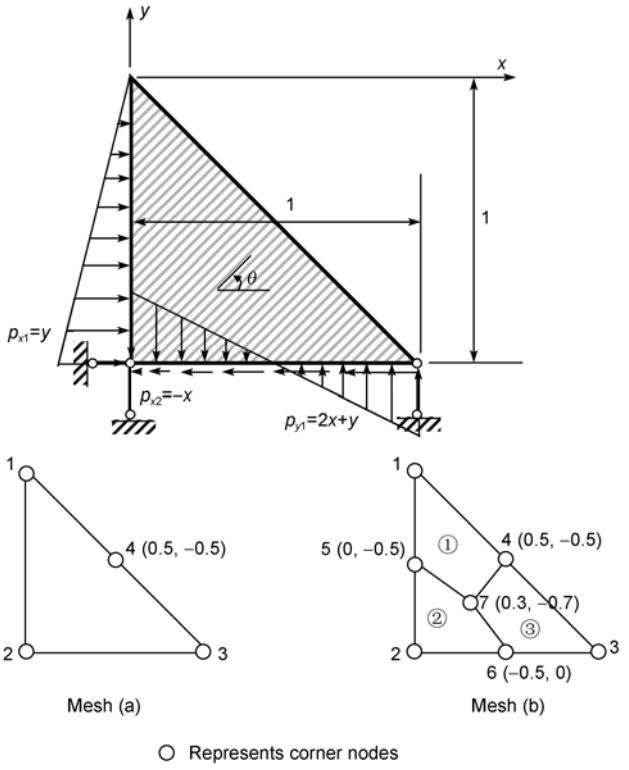

Figure 4 A triangular orthotropic patch subjected to linearly distributed loads.

6 Conclusions

The finite element method has been suffering from the sensitivity problem to mesh distortion for a long time. In this work, by applying the fundamental analytical solutions (in global Cartesian coordinates) to the Airy stress function ϕ of the anisotropic materials, 8- and 12-node plane quadrilateral hybrid stress-function (HS-F) elements are successfully developed based on the principle of the minimum complementary energy. Numerical results show that the present new elements exhibit excellent performance: They can perform very well in severe distorted meshes, even when the element shape degenerates into a triangle and a concave quadrangle. It is also demonstrated that the proposed construction procedure is an effective way for developing shape-free finite element models which can completely overcome the sensitivity problem to mesh distortion.

The element with a concave shape should not be directly used at the concave boundary unless the corresponding singular solutions are considered in the trial functions.

This work was supported by the National Natural Science Foundation of China (Grant No.10872108, 10876100), the Program for New Century Excellent Talents in University (Grant No. NCET-07-0477), the National Basic Research Program of China (Grant No. 2010CB832701), and ASFC.

1 Zienkiewicz O C, Taylor R L, Zhu J Z. The Finite Element Method: Its Basis & Fundamental. 6th ed. Butterworth Heinemann: Elsevier, 2005
2 Long Y Q, Cen S, Long Z F. Advanced Finite Element Method in Structural Engineering. Berlin, Heidelberg: Springer-Verlag GmbH; Beijing: Tsinghua University Press, 2009
3 Lee N S, Bathe K J. Effects of element distortion on the performance of isoparametric elements. Int J Numer Methods Eng, 1993, 36: 3553–3576. DOI: 10.1002/nme.1620362009
4 Wilson E L, Tayler R L, Doherty WP, et al. Incompatible displacement models. Fenves S J, et al, eds. Numerical and Computational Methods in Structural Mechanics, New York: Academic Press, 1973. 43–57
5 Taylor R L, Beresford P J, Wilson E L. A non-conforming element for stress analysis. Int J Numer Methods Eng, 1976, 10: 1211–1219. DOI: 10.1002/nme.1620100602
6 Ibrahimbegovic A, Wilson E L. A modified method of incompatible modes. Commun Appl Numer Methods, 1991, 7: 187–194. DOI: 10.1002/cnm.1630070303

7 Simo J C, Rifai M S. A class of mixed assumed strain methods and the method of incompatible modes. Int J Numer Methods Eng, 1990, 29: 1595–1638. DOI: 10.1002/nme.1620290802

8 Belytschko T, Bachrach W E. Efficient implementation of quadrilaterals with high coarse-mesh accuracy. Comput Methods Appl Mech Eng, 1986, 54: 279–301. DOI: 10.1016/0045-7825(86)90107-6

9 Hughes T J R. Generalization of selective integration procedures to anisotropic and nonlinear media. Int J Numer Methods Eng, 1980, 16: 1413–1418. DOI: 10.1002/nme.1620150914

10 Macneal R H. Derivation of element stiffness matrices by assumed strain distributions. Nucl Eng Des, 1982, 70: 3–12. DOI: 10.1016/0029-5493(82)90262-X

11 Piltner R, Taylor R L. A systematic construction of B-bar functions for linear and nonlinear mixed-enhanced finite elements for plane elasticity problems. Int J Numer Methods Eng, 1999, 44: 615–639. DOI:10.1002/(SICI)1097-0207(19990220)44:5<615::AID-NME518>3.0.CO;2-U

12 Tang L M, Chen W J, Liu Y G. Formulation of quasi-conforming element and Hu-Washizu principle. Comput Struct, 1984, 19: 247–250. DOI:10.1016/0045-7949(84)90224-4

13 Long Y Q, Huang M F. A generalized conforming isoparametric element. Appl Math Mech, 1988, 9: 929–936. DOI: 10.1007/BF02014599

14 Liu G R, Nguyen-Thoi T, Lam K Y. A novel FEM by scaling the gradient of strains with factor α (αFEM). Comput Mech, 2009, 43: 369–391. DOI: 10.1007/s00466-008-0311-1

15 Chen J, Li C J, Chen W J. A family of spline finite elements. Comput Struct, 2010, 88: 718–727. DOI: 10.1016/j.compstruc.2010.02.011

16 Rajendran S, Liew K M. A novel unsymmetric 8-node plane element immune to mesh distortion under a quadratic displacement field. Int J Numer Methods Eng, 2003, 58: 1713–1748. DOI: 10.1002/nme.836

17 Ooi E T, Rajendran S, Yeo J H. A 20-node hexahedron element with enhanced distortion tolerance. Int J Numer Methods Eng, 2004, 60: 2501–2530. DOI: 10.1002/nme.1056

18 Rajendran S. A technique to develop mesh-distortion immune finite elements. Comput Methods Appl Mech Eng, 2010, 199: 1044–1063. DOI:10.1016/j.cma.2009.11.017

19 Long Y Q, Li J X, Long Z F, et al. Area coordinates used in quadrilateral elements. Commun Numer Methods Eng, 1999, 15: 533–545 DOI:10.1002/(SICI)1099-0887(199908)15:8<533::AID-CNM265>3.0.CO;2-D

20 Long Z F, Li J X, Cen S, et al. Some basic formulae for area coordinates used in quadrilateral elements. Commun Numer Methods Eng, 1999, 15: 841–852. DOI: 10.1002/(SICI)1099-0887(199912)15: 2<841::AID-CNM290>3.0.CO;2-A

21 Chen X M, Cen S, Long Y Q, et al. Membrane elements insensitive to distortion using the quadrilateral area coordinate method. Comput Struct, 2004, 82: 35–54. DOI: 10.1016/j.compstruc.2003.08.004

22 Chen X M, Cen S, Fu X R, et al. A new quadrilateral area coordinate method (QACM-II) for developing quadrilateral finite element models. Int J Numer Methods Eng, 2008, 73: 1911–1941. DOI: 10.1002/nme.2159

23 Long Z F, Cen S, Wang L, et al. The third form of the quadrilateral area coordinate method (QACM-III): theory, application, and scheme of composite coordinate interpolation. Finite Elem Anal Des, 2010, 46: 805–818. DOI: 10.1016/j.finel.2010.04.008

24 Li H G, Cen S, Cen Z Z. Hexahedral volume coordinate method (HVCM) and improvements on 3D Wilson hexahedral element. Comput Methods Appl Mech Eng, 2008, 197: 4531–4548. DOI: 10.1016/j.cma.2008.05.022

25 Belytschko T, Lu Y Y, Gu L. Element free Galerkin methods. Int J Numer Methods Eng, 1994, 37: 229–256. DOI: 10.1002/nme.1620370205

26 Atluri S N, Zhu T. A new meshless local Petrov-Galerkin (MLPG) approach in computational mechanics. Comput Mech, 1998, 22: 117–127. DOI: 10.1007/s004660050346

27 Zhang X, Liu X H, Song K Z, et al. Least-squares collocation meshless method. Int J Numer Methods Eng, 2001, 51: 1089–1100. DOI: 10.1002/nme.200

28 Zhang J M, Yao Z H, Li H. A hybrid boundary node method. Int J Numer Methods Eng, 2002, 53: 751–763. DOI: 10.1002/nme.313

29 Cai Y C, Zhu H H. A PU-based meshless Shepard interpolation method satisfying delta property. Eng Anal with Bound Elem, 2010, 34: 9–16. DOI:10.1016/j.enganabound.2009.07.007

30 Pian T H H. Derivation of element stiffness matrices by assumed stress distributions. AIAA J, 1964, 2: 1333–1336

31 Fu X R, Cen S, Li C F, et al. Analytical trial function method for development of new 8-node plane element based on the variational principle containing airy stress function. Engineering Computations, 2010, 27: 442–463. DOI: 10.1108/02644401011044568

32 Cen S, Fu X R, Zhou M J. A novel hybrid stress-function finite element method immune to severe mesh distortion. In: IOP Conference Series: Materials Science and Engineering (Proceedings of WCCM/APCOM 2010), 2010, 10: 012220. DOI: 10.1088/1757-899X/10/1/012220

33 Teixeira de Freitas J A. Formulation of elastostatic hybrid-Trefftz stress elements. Comput Methods Appl Mech Eng, 1998, 153: 127–151. DOI:10.1016/S0045-7825(97)00042-X

34 Freitas J A T, Wang Z M. Hybrid-Trefftz stress elements for elastoplasticity. Int J Numer Methods Eng, 1998, 43: 655–683. DOI: 10.1002/(SICI)1097-0207(19981030)43:4<655::AID-NME416>3.0.CO;2-1

35 Freitas J A T, Bussamra F L S. Three-dimensional hybrid - Trefftz stress elements. Int J Numer Methods Eng, 2000, 47: 927–950. DOI: 10.1002/(SICI)1097-0207(20000220)47:5<927::AID-ME805>3.0.CO;2-B